Mon. Not. R. Astron. Soc. **394,** 2229–2237 (2009) doi:10.1111/j.1365-2966.2009.14491.x

The influence of halo assembly on galaxies and galaxy groups

Tatiana Zapata,[1,2]★ Josefa Perez,[3] Nelson Padilla[1] and Patricia Tissera[3]

[1]*Departamento de Astronomía y Astrofísica, Pontificia Universidad Católica de Chile, Santiago, Chile*
[2]*Instituto de Astronomia, Geofísica e Ciências Atmosféricas, Universidade de São Paulo, Brasil*
[3]*Instituto de Astronomía y Física del Espacio, Conicet-UBA, CC67, Suc. 28, Ciudad de Buenos Aires, Argentina*

Accepted 2009 January 12. Received 2009 January 6; in original form 2008 April 27

ABSTRACT

In this paper, we study the variations of group galaxy properties according to the assembly history in Sloan Digital Sky Survey Data Release 6 (SDSS-DR6) selected groups. Using mock SDSS group catalogues, we find two suitable indicators of group formation time: (i) the isolation of the group, defined as the distance to the nearest neighbour in terms of its virial radius and (ii) the concentration, measured as the group inner density calculated using the fifth nearest bright galaxy to the group centre. Groups within narrow ranges of mass in the mock catalogue show increasing group age with isolation and concentration. However, in the observational data the stellar age, as indicated by the spectral type, only shows a correlation with concentration.

We study groups of similar mass and different assembly history, finding important differences in their galaxy population. Particularly, in high-mass SDSS groups, the number of members, mass-to-light ratios, red galaxy fractions and the magnitude difference between the brightest and second-brightest group galaxies, show different trends as a function of isolation and concentration, even when it is expected that the latter two quantities correlate with group age. Conversely, low-mass SDSS groups appear to be less sensitive to their assembly history.

The correlations detected in the SDSS are not consistent with the trends measured in the mock catalogues. However, discrepancies can be explained in terms of the disagreement found in the age-isolation trends, suggesting that the model might be overestimating the effects of environment. We discuss how the modelling of the cold gas in satellite galaxies could be responsible for this problem. These results can be used to improve our understanding of the evolution of galaxies in high-density environments.

Key words: galaxies: clusters: general – galaxies: general.

1 INTRODUCTION

Up to only a few years back, the mass of a dark matter halo was the only parameter considered to affect its clustering properties in an important or detectable way (see e.g. Mo & White 1996; Sheth, Mo & Tormen 1998; Padilla & Baugh 2002) as well as the galaxy population inside haloes. The latter has been studied in the framework of the halo model (Cooray & Sheth 2002; Cooray 2005, 2006 and references therein), whereby the number of galaxies per dark matter halo, as well as central and satellite luminosities and possibly colours, is proposed to depend only on the host halo mass (Wang et al. 2008); by assuming this, most of the global fundamental statistics of the galaxy population can then be reproduced.

Recent studies on the clustering of dark matter haloes found that the age and assembly history of haloes of similar mass influence their clustering amplitude. The dependence on halo age was first reported by Gao, Springel & White (2005), and has been studied into more detail finding a general dependency on the way in which a halo is assembled by Gao & White (2007), Jing, Suto & Mo (2007), Croton, Gao & White (2007) and Wechsler et al. (2007). The assembly bias has also been detected in observations by Wang et al. (2008); their studies only concentrate on the clustering amplitude of different samples selected according to group colour which they associate with group age.

Our aim is to detect the effects of halo assembly on the galaxy population. Note that even though there have been several attempts to study the environmental dependence of galaxy properties in the Sloan Digital Sky Survey (SDSS; as e.g. in Blanton & Berlind 2007; O'Mill, Padilla & Lambas 2008), and other galaxy catalogues [in the two-degree Field Galaxy Redshift Survey (2dFGRS) by González et al. 2005], none of these works relates their results to the influence of halo assembly. In addition to using group colour as an indicator of halo age, we will explore other parameters as indicators such as

★E-mail: taz@astro.iag.usp.br

the degree of dynamical relaxation of a group given by its apparent projected shape (rounder objects tend to be older; see Paz et al. 2006) or concentration (Gao & White 2007; Wechsler et al. 2007), luminosity difference between the brightest and second-brightest galaxies in the group (used to identify old, fossil groups; Mendes de Oliveira & Carrasco 2007; von Benda-Beckmann et al. 2007) and group isolation.

This paper is organized as follows. Section 2 presents the sets of observational data used in this work as well as the mock catalogues constructed from semi-analytic galaxies. In Section 3, we explore different indicators of group age. Section 4 shows the variations of galaxy properties as a function of group isolation and concentration. Section 5 presents a discussion and Section 6 summarizes the main results of this work.

2 DATA

2.1 Observations

We use the SDSS Data Release 6 (SDSS-DR6; Adelman-McCarthy et al. 2007) to identify groups following the prescription presented by Merchán & Zandivarez (2005), which consists of a friends-of-friends (FOF) algorithm with varying projected linking length σ, with $\sigma_0 = 0.239\,h^{-1}$ Mpc and fixed radial linking length $\Delta v = 450\,\mathrm{km\,s^{-1}}$. These parameters correspond to the values found by Merchán & Zandivarez to produce a reasonably complete sample with low contamination (95 and $\lesssim$8 per cent, respectively). The minimum number of galaxies per group in our sample is set to 10.

Even though there are previous compilations of groups in the SDSS such as the catalogues compiled from the SDSS-DR3 (Merchán & Zandivarez 2005) and DR4 (Yang et al. 2007), and by using percolation algorithms (Berlind et al. 2006) on the New York University Value Added Catalogue (NYU-VAGC) (Blanton et al. 2005), we need to perform our own identification in order to control the measurements of group centre, mass and membership. Furthermore, given the low statistical significance and high susceptibility to observational biases, we also need mock catalogues on which to perform our analyses to test for these effects. Therefore, we apply exactly the same group detection algorithm to a SDSS mock catalogue which we will describe in the following section.

We use the virial theorem to compute the virial mass of groups which is given by

$$M_{\rm vir} = \frac{3\sigma_v^2 R_{\rm vir}}{G}, \tag{1}$$

where σ_v is the line-of-sight velocity dispersion and $R_{\rm vir}$ is estimated as in Merchán & Zandivarez (2005),

$$R_{\rm vir} = \frac{\pi}{2}\frac{N_{\rm g}(N_{\rm g}-1)}{\Sigma_{i>j} R_{ij}^{-1}}, \tag{2}$$

where $N_{\rm g}$ is the number of galaxy members and R_{ij} are the galaxy relative projected distances.

Throughout this paper, the quoted errors in measurements involving SDSS groups will correspond to errors in the mean obtained using the jacknife technique with 10 subsamples.

2.2 Mock catalogues

We construct a mock SDSS catalogue using the semi-analytic model (SAM) from De Lucia et al. (2006), who use the merger trees from the Millennium Simulation (Springel et al. 2005) to follow different physical processes that lead to the final $z = 0$ galaxy population in a Λ cold dark matter cosmology, with cosmological parameters determined from the combined analysis of the 2dFGRS (Colles et al. 2001) and the first-year *Wilkinson Microwave Anisotropy Probe* (*WMAP*) data (Spergel et al. 2003): $\Omega_{\rm m} = 0.25$; $\Omega_{\rm b} = 0.045$; $\Omega_\Lambda = 0.75$; $h = 0.73$; $n = 1$ and $\sigma_8 = 0.9$. The Millennium Simulation consists of 2160^3 particles, in a box of $500\,h^{-1}$ Mpc on a side, with a particle mass resolution of $8.6 \times 10^8\,h^{-1}\,\mathrm{M}_\odot$. The resulting galaxies conform a complete sample down to a magnitude $M_r = -16$.

In order to mimic the SDSS, we place four observers on different locations in the $z = 0$ output from the numerical simulation so that the volumes surveyed by each observer are as independent as possible; this is achieved by placing observers in the centre of four opposite octants in a diagonal direction, with two of the observers (on a long diagonal) facing in a direction offset by 90° (in the $x - y$ and $y - z$ planes) with respect to the other two observers. The minimum distance between observers is $\simeq 350\,h^{-1}$ Mpc, and they sample different regions of the simulation in different directions. We apply the same angular mask affecting the spectroscopic main sample, and apply a magnitude limit cut of $r_{\rm lim} = 17.77$. For each galaxy, we store its observed properties, such as redshift (which includes the peculiar motion), angular position in the sky and apparent magnitudes in several bands. However, the main advantage of the mock catalogue is that we also store several intrinsic properties such as luminosity in different bands and properties of the host halo including its mass.

We apply the adaptive FOF algorithm to each mock SDSS catalogue, using exactly the same search parameters applied to the real data. In this way, we obtain four mock group catalogues which are studied the same way as the real SDSS groups; in particular, we use the same minimum number of galaxies per group, as well as the same method to estimate group masses.

In the remainder of this paper, the results obtained from the mocks will correspond to the average over our four mock SDSS catalogues; the uncertainties represented by the error bars will correspond to the errors in the mean obtained using the jacknife technique with 10 subsamples, averaged over the mock catalogues.

3 SEARCHING FOR OBSERVATIONAL INDICATORS OF GROUP ASSEMBLY

In this section, we analyse the variation of galaxy group properties with the aim of finding an indicator of group age which can be related to the assembly history of the group host halo. We will analyse several candidates of observational parameters that will allow us to rank our observational and simulated group samples according to their assembly history.

In the case of the mock catalogues, the group age is directly estimated by the mean stellar-mass-weighted age of the galaxies hosted by a given group. The star formation histories of galaxies in groups are determined by the rate of gas consumption which is modulated by the assembly history of the haloes (i.e. collapse, infall, mergers) and feedback mechanisms which in effect are regulated by the size of the haloes. A recent work by Li, Mo & Gao (2008) shows that a halo age related to the formation history of its member galaxies is the most appropriate for detecting the assembly effects on the bias parameter; in this case, the effect is seen for all halo masses, including the ranges we will study in this paper, $12.9 < \log_{10}(M_{\rm vir}\,h^{-1}\,\mathrm{M}_\odot) < 14.0$. This justifies our choice of halo age indicator.

Observationally, this parameter is more complicated to estimate. In order to find the best observational indicator which could be

related to group age, we first search for possible correlations between the mock group ages and other group parameters.

Although the first candidate for age that comes to mind is the group mass as larger groups started to collapse earlier (see e.g. Paz et al. 2006), our aim is to explore any possible variation of group properties with age for fixed values of group mass. Hence, for fixed group masses, we test a series of observable parameters.

(i) The projected group shape measured by the ratio between the minor and major semi-axes of an ellipse such that the eigenvalues of the anisotropic part of its inertia tensor are the same as obtained from the projected positions of the group members.

(ii) The difference in magnitudes between the first and second-brightest galaxies in the group (ΔM_{12}).

(iii) The fraction of red galaxies in the group ($u - r \geq 2.0$).

(iv) The degree of isolation of a group defined as the distance $D_{\rm neighbour}/R_{\rm vir}$ (measured in terms of the group virial radius) to the nearest group neighbour,.

(v) The concentration measured by the group inner density (Σ_5), calculated by using the projected distance to the fifth galaxy, brighter than $M_r = -20.5$.

(vi) The mass-to-light ratio which we obtain using luminosities measured in the *r* band.

We find that the group shape is not a good indicator of group age due to the lack of statistical significance of a relation between them. Conversely, the fraction of red galaxies, the *M/L* ratio, $D_{\rm neighbour}/R_{\rm vir}$ and Σ_5 show clear correlations with mean stellar-mass-weighted ages as it can be appreciated in Fig. 1. In all cases, we divide the group catalogues into subsamples defined by two narrow (0.4 dex wide) ranges of halo mass: high-mass groups selected within $13.6 < \log_{10}(M_{\rm vir}\, h^{-1}\, {\rm M}_\odot) < 14.0$ and low-mass groups within $12.9 < \log_{10}(M_{\rm vir}\, h^{-1}\, {\rm M}_\odot) < 13.3$ (from this point on, we will use the same halo mass ranges to study galaxy group properties as a function of different age indicators).

Even though there is also a clear trend of age with the fraction of red galaxies and the mass-to-light ratio, it has been shown that SAMs overestimate the fraction of red galaxies (e.g. Weinmann et al. 2006). Conversely, the trends with group concentration and isolation are very well defined, showing that for the model the most isolated and concentrated groups tend to be older. Since these parameters are more directly related to the structure of the dark matter, we adopt both estimators as good indicators of group age and assembly history. As it can be seen from the lower panels of Fig. 1, a semi-analytic galaxy group with no neighbour groups out to 10 times its virial radius, or with an internal density larger than

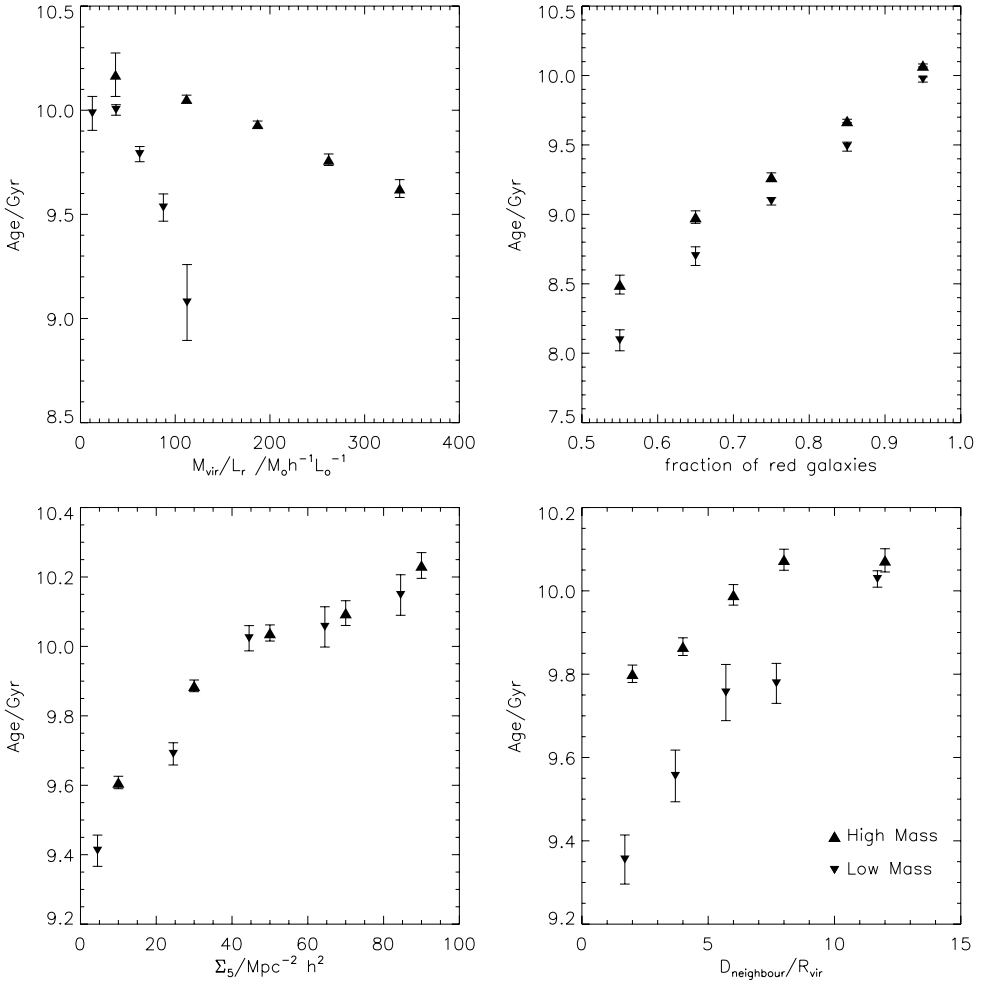

Figure 1. Dependence of halo age on mass-to-light ratio (top-left panel), fraction of red galaxies (top-right panel), on group inner density using the five brightest galaxies in the group (bottom-left panel) and isolation in terms of the group virial radius (bottom-right panel) in the mock catalogues. All panels show the relations for two different narrow (0.4 dex wide) ranges of halo mass; upward pointing triangles correspond to high masses, $13.6 < \log_{10}(M_{\rm vir}\, h^{-1}\, {\rm M}_\odot) < 14.0$ and downward triangles to low masses, $12.9 < \log_{10}(M_{\rm vir}\, h^{-1}\, {\rm M}_\odot) < 13.3$.

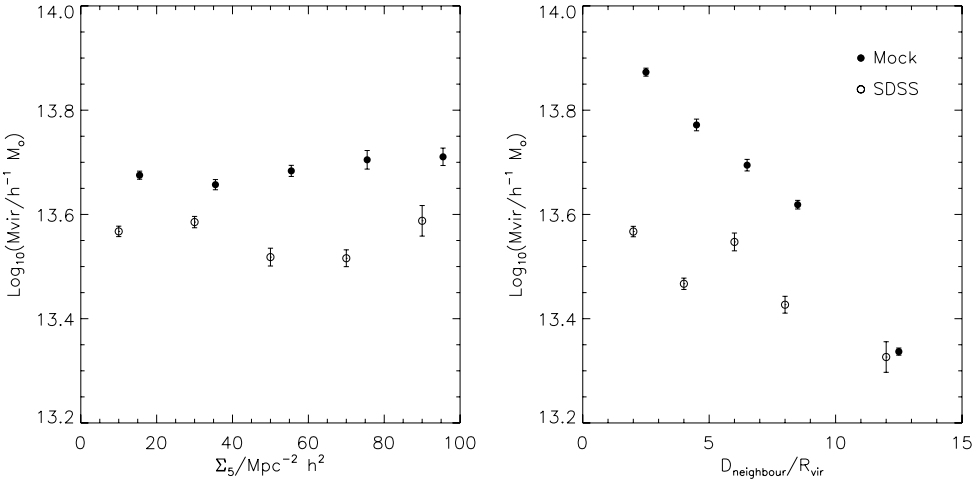

Figure 2. Dependence of group mass on concentration (right-hand panel) and group isolation (left-hand panel) for groups in the SDSS and mock catalogues.

$80\,h^2\,\mathrm{Mpc}^{-2}$, is likely to be up to 800 Myr older than a group living in a more populated area or with a lower concentration.

This analysis also shows that both group age indicators (isolation and concentration) depend on halo mass. In fact, in Fig. 2 we plot halo mass as a function of concentration (left-hand panel) and isolation (right-hand panel) for the mock (solid symbols) and the SDSS (open symbols). Both the observations and model show a trend with both parameters, however the dependence of mass on concentration is very weak, indicating that the concentration may be better suited to study assembly effects without introducing biases. Nevertheless, given that the isolation of a group can store information on its large-scale neighbourhood, we will also include it in our analysis.

In order to detect dependencies of different group properties on these two age indicators, we will separate groups according to the proposed age parameter in two bins corresponding to young and old objects. Then for each bin, we calculate the mean group properties and errors using the jacknife technique, and characterize the statistical significance of a trend by quoting the resulting difference between the galaxy population property in old and young groups (χ^2). Note that for one degree of freedom, $\chi^2 = n$ indicates a $n\sigma$ detection. In the case of concentration, we will consider as old objects those characterized by $\Sigma_5 \geq 70\,h^2\,\mathrm{Mpc}^{-2}$ and as young objects those with $\Sigma_5 \leq 30\,h^2\,\mathrm{Mpc}^{-2}$. The limits for the case of isolation are set to $D_{\mathrm{neighbour}}/R_{\mathrm{vir}} \geq 8$ for old objects and $D_{\mathrm{neighbour}}/R_{\mathrm{vir}} \leq 7$ for young objects. One important advantage of this approach is that correlations between different isolation or concentration bins are reduced to a minimum.

A possible equivalent observational estimator of stellar mass age is the galaxy spectral type (Yip et al. 2004); lower values of spectral type correspond to earlier galaxy types and, therefore, to older stellar populations. In a similar way, spectral types correlate with colours, corresponding to a value of -0.08 for the limit spectral type which separates the red and blue sequences. In order to test the validity of the previous theoretical indicators of age, Fig. 3 shows the mean spectral type of SDSS groups as a function of concentration (left-hand panel) and isolation (right-hand panel). For massive groups, we find different trends with these parameters. While higher concentration massive SDSS groups are populated with systematically lower spectral type (i.e. older stellar populations, 4.85σ effect; see Table 1), the more isolated massive groups contain somewhat higher spectral type galaxies (i.e. younger, 1.39σ effect; see Table 1). These correlations show that SDSS groups confirm the predicted correlation between concentration and age found in mock catalogues (Fig. 1). However, a disagreement in the SDSS

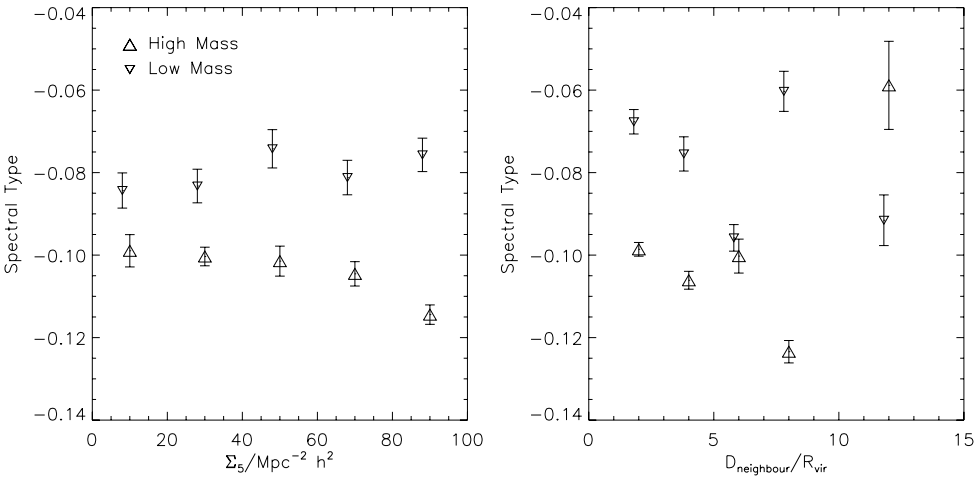

Figure 3. Average group spectral type as a function of group concentration (left-hand panel) and isolation (right-hand panel) for groups in the SDSS separated according to the estimated virial mass as high (upward pointing triangles) and low (downward pointing triangles) group masses (see Fig. 1).

Table 1. SDSS results: significance of trends in spectral type (column 3), mass-to-light ratios (column 4), occupation numbers (column 5), fraction of red galaxies (column 6) and magnitude difference between brightest and second-brightest group member (column 7), as a function of concentration (top rows) and isolation (bottom rows).

Mass range	Quantity	Spectral type	$M_{\rm vir}/L_r/({\rm M}_\odot\, h^{-1}\, {\rm L}_\odot^{-1})$	$\log_{10}(N_{\rm gal})$	Red galaxy fractions	ΔM_{12}
High mass	Low Σ_5	-0.097 ± 0.002	572 ± 13	1.178 ± 0.032	0.784 ± 0.004	0.49 ± 0.04
	High Σ_5	-0.108 ± 0.001	443 ± 8	1.454 ± 0.053	0.809 ± 0.005	0.54 ± 0.04
	χ^2 (trend)	4.85 (decr.)	8.37 (decr.)	4.47 (incr.)	4.02 (incr.)	0.9 (none)
Low mass	Low Σ_5	-0.08 ± 0.002	180 ± 3	1.065 ± 0.017	0.77 ± 0.01	0.49 ± 0.06
	High Σ_5	-0.077 ± 0.002	158 ± 5	1.064 ± 0.013	0.815 ± 0.006	0.64 ± 0.04
	χ^2 (trend)	1.07 (incr.)	3.94 (decr.)	0.006(none)	3.84 (incr.)	1.99 (incr.)
High mass	Low $D_{\rm neighbour}/R_{\rm vir}$	-0.099 ± 0.001	498 ± 13	1.302 ± 0.021	0.809 ± 0.005	0.45 ± 0.01
	High $D_{\rm neighbour}/R_{\rm vir}$	-0.091 ± 0.006	704 ± 40	1.121 ± 0.038	0.763 ± 0.016	0.51 ± 0.05
	χ^2 (trend)	1.39 (incr.)	4.92 (incr.)	7.9 (decr.)	2.7 (decr.)	1.18 (incr.)
Low mass	Low $D_{\rm neighbour}/R_{\rm vir}$	-0.0735 ± 0.001	227 ± 6	1.086 ± 0.014	0.797 ± 0.004	0.44 ± 0.02
	High $D_{\rm neighbour}/R_{\rm vir}$	-0.0733 ± 0.003	144 ± 3	1.069 ± 0.027	0.749 ± 0.007	0.52 ± 0.02
	χ^2 (trend)	0.06 (none)	11.51 (decr.)	8.02 (decr.)	5.33 (decr.)	2.53 (incr.)

Note. All quantities are rounded to $\sim$1 significant figure in the error, estimated using the jacknife technique.

and mock isolation age/spectral type trends reveals that the model may be overestimating the effects of environment. We will come back to this point in the following sections. On the other hand, low-mass SDSS groups show no significant trend (at most 1σ), with either isolation or concentration, again in contradiction to the findings obtained from the mock catalogues.

In the following section, we turn to the study of the variation of galaxy group properties as a function of assembly epoch as indicated by group concentration and isolation. When using isolation as an age indicator, we bear in mind the differences between observations and models.

4 GALAXY GROUP PROPERTIES AS A FUNCTION OF GROUP AGE

In principle, halo models (cf. Cooray & Sheth 2002) and the conditional luminosity function (Cooray 2005, 2006) are able to establish the properties of galaxies in dark matter haloes using only the halo mass. This technique has been very successful in reproducing several galaxy statistics such as the correlation function of SDSS galaxies (Zehavi et al. 2004) and numerical simulations (Zheng et al. 2005), and the evolution of the luminosity function of galaxies up to $z = 6$ (Cooray 2005). However, as we will show in this section, the properties of galaxies in groups of similar masses are also dependent on the concentration and isolation of the group, parameters related to the assembly history of the system.

We start analysing the variations of mass-to-light ratios, *M*/*L*, of low- and high-mass groups for different degrees of isolation and concentration. Fig. 4 shows the *M*/*L* ratios as a function of group concentration (left-hand panel) and isolation (right-hand panel). In consistency with our previous result for spectral types, high-mass SDSS groups show two clear opposite trends of decreasing (8.37σ; Table 1) and increasing M/L (4.92σ; Table 1) with concentration and isolation, respectively, of almost a 50 per cent change. As can be seen, both trends are comparatively significant. A more detailed analysis shows that (90 ± 10) per cent of the *M*/*L* ratios exhibited by groups isolated by more than eight virial radii lies above the median relation between *M*/*L* ratio to Σ_5; however, the values of Σ_5 for these isolated groups span almost the entire range of concentrations shown in the figure. This tells us that more isolated groups at a given concentration show higher *M*/*L* ratios. Note also that since the analysis is carried out in a narrow mass range, the increase or decrease in *M*/*L* can be directly related to a decrease or increase, respectively, in the *r*-band luminosity. Therefore, the opposite

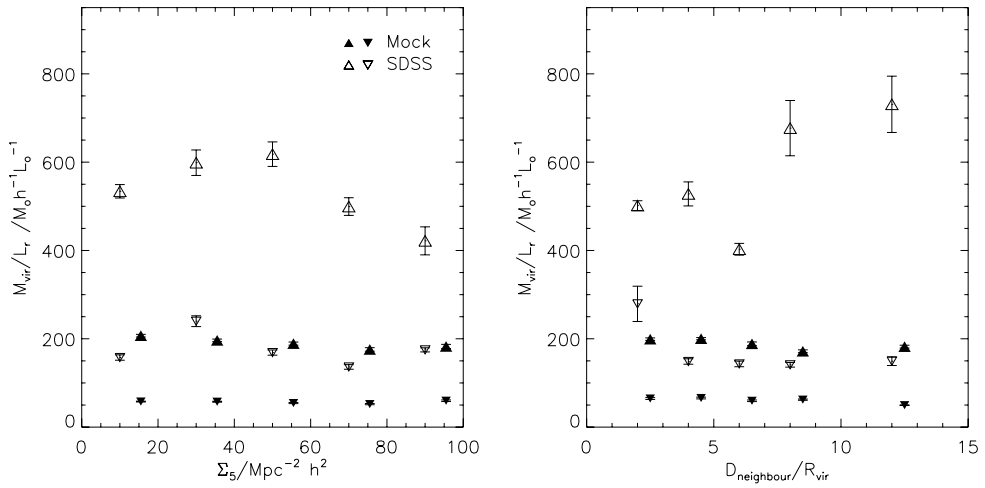

Figure 4. Dependence of mass-to-light ratios on group concentration (left-hand panel) and isolation (right-hand panel) for mock and SDSS (filled and open symbols, respectively) groups, in two narrow ranges of halo mass (high masses are shown in upward pointing triangles, low masses in downward triangles).

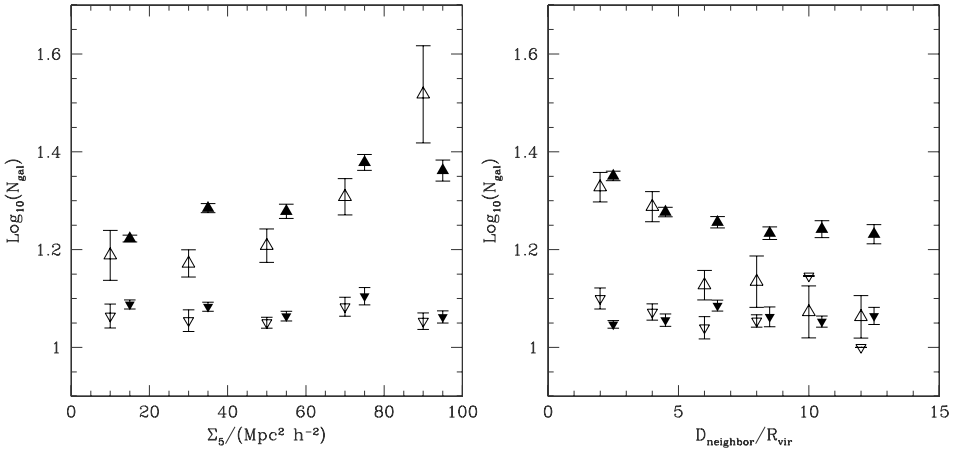

Figure 5. Dependence of the number of galaxy members on group concentration (left-hand panel) and isolation (right-hand panel) for mock and SDSS-DR6 groups (filled and open symbols, respectively), in two narrow ranges of halo mass (high masses are shown in upward pointing triangles, low masses in downward triangles).

behaviours in the *M*/*L* ratios observed for the SDSS high-mass groups with concentration and isolation can also be associated to opposing trends in their *r*-band luminosities. This can be explained in terms of their spectral types; while high-mass SDSS groups tend to be older with increasing concentration (and consequently brighter in the *r* band), they tend to be younger with increasing isolation (and fainter in the same band).

On the other hand, Fig. 4 also shows that low-mass SDSS groups exhibit compatible trends of decreasing *M*/*L* with both concentration and isolation, with a high statistical significance (Table 1). Interestingly, groups in the mock catalogues show this trend for both high- and low-mass groups (the mass-to-light ratios decrease as a function of isolation and concentration). This discrepancy between observational and mock catalogues for high-mass groups is an indication of possible problems in the modelling of the physical processes associated to the baryonic component in the SAM, since the mass-to-light ratio, *M*/*L*, is strongly dependent on the galaxy population.

In order to investigate further the origin of these behaviours, we also estimate the number of group members as a function of concentration and isolation, for both SDSS and mock groups. As it can be seen in Fig. 5, the number of members for high-mass SDSS groups decreases with isolation (7.9σ; Table 1) and increases with concentration (4.47σ; Table 1). This result is also consistent with the *M*/*L* and *r*-band luminosity tendencies since a decreasing number of members produce lower total luminosities as the group isolation increases and an increasing number of galaxy members result in higher luminosities as the concentration increases. Note that, although high-mass groups in the mock catalogues exhibit similar trends than the observations (see Table 2) for the number of galaxy members as a function of concentration and isolation (Fig. 5), they totally disagree in reproducing the *M*/*L* behaviour. This suggests that the intrinsic luminosity of the galaxy members varies differently in the model and observations as a function of isolation and concentration. This discrepancy between mock and SDSS groups may be an indication that the model fails in describing the physical processes associated to the baryonic component to some level. Several facts could be involved: there could be an offset in the gas accretion rates on to the halo; the star formation time-scales could be too short; the threshold cold gas surface density for star formation could be too low; the suppression of star formation by active galactic nuclei (AGN) heating could be overestimated; the merging time-scales could be too short; environmental effects could be exacerbated and so on. Because the most significant discrepancy is observed for the most massive haloes in low-density environments (large isolation), we can rule out some of these sources of disagreement. In the perspective of the current hierarchical model of structure formation, where massive haloes assemble rather late through the merging of smaller systems, gas cooling processes are the main contributors to the galaxy mass growth in low-mass haloes. On the other hand, galaxy–galaxy mergers are more efficient within small haloes with low velocity dispersion. As a consequence, both

Table 2. Mock results: columns and rows are as in Table 1.

Mass range	Quantity	Spectral type	$M_{\rm vir}/L_r/({\rm M}_\odot\,h^{-1}\,{\rm L}_\odot^{-1})$	$Log_{10}(N_{\rm gal})$	Red galaxy fractions	ΔM_{12}
High mass	Low Σ_5	N/A	202 ± 2	1.231 ± 0.006	0.863 ± 0.002	0.70 ± 0.01
	High Σ_5	N/A	177 ± 2	1.379 ± 0.013	0.913 ± 0.002	0.77 ± 0.03
	χ^2 (trend)	N/A	10.3 (decr.)	10.0 (incr.)	17.6 (incr.)	2.23 (incr.)
Low mass	Low Σ_5	N/A	60 ± 1.6	1.088 ± 0.008	0.854 ± 0.005	0.61 ± 0.02
	High Σ_5	N/A	56 ± 1.7	1.087 ± 0.014	0.938 ± 0.006	0.67 ± 0.03
	χ^2 (trend)	N/A	1.9 (decr.)	0.09 (none)	11.4 (incr.)	1.45 (incr.)
High mass	Low $D_{\rm neighbour}/R_{\rm vir}$	N/A	198 ± 2	1.313 ± 0.006	0.881 ± 0.002	0.75 ± 0.01
	High $D_{\rm neighbour}/R_{\rm vir}$	N/A	177 ± 2	1.227 ± 0.009	0.921 ± 0.002	0.73 ± 0.02
	χ^2 (trend)	N/A	7.2 (decr.)	8.1 (decr.)	11.28 (incr.)	0.86 (none)
Low mass	Low $D_{\rm neighbour}/R_{\rm vir}$	N/A	64 ± 1.1	1.062 ± 0.006	0.852 ± 0.01	0.64 ± 0.02
	High $D_{\rm neighbour}/R_{\rm vir}$	N/A	53 ± 0.7	1.07 ± 0.01	0.916 ± 0.002	0.64 ± 0.02
	χ^2 (trend)	N/A	8.7 (decr.)	0.67 (none)	8.4 (incr.)	0.08 (none)

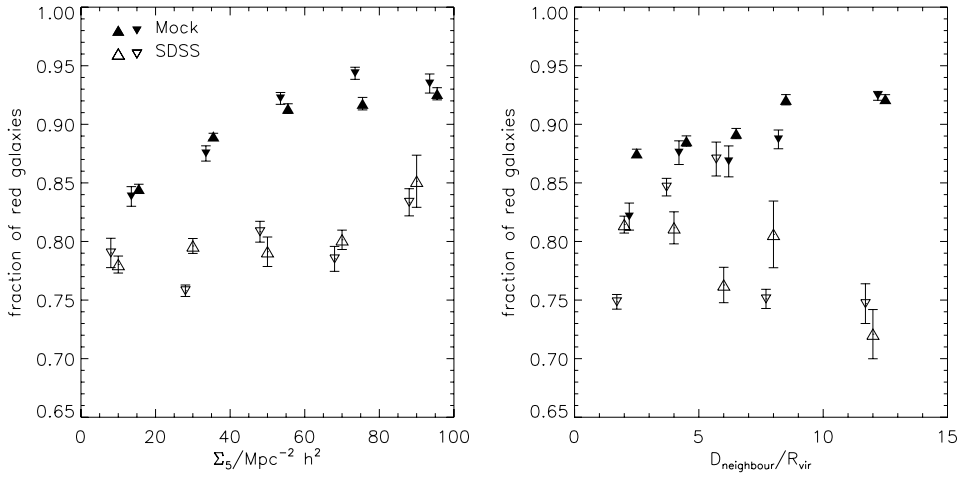

Figure 6. Dependence of the red galaxy fraction on concentration (left-hand panel) and isolation (right-hand panel) for mock (filled symbols) and SDSS (open symbols) groups in two narrow ranges of mass (low masses indicated by downward pointing triangles, high masses by upward triangles).

processes would not explain the observed disagreement. AGN feedback acts regulating the star formation activity in massive galaxies and has been proved to be reasonably well suited to reproduce several observational statistics, so it is not likely to be responsible for the present problem. Thus, the remaining possible causes could lie in the star formation prescription or in environmental processes. Recently, analytic and hydrodynamic simulations have shown that the environment in groups and cluster is less aggressive than previously assumed. It has been argued that the excess of red satellite owes to an oversimplified treatment of ram pressure stripping of their hot gaseous haloes. In general, SAMs assume that the entire hot gas reservoir of a galaxy is instantaneously stripped at the moment of accretion into a larger halo (when it becomes a satellite galaxy). Recent improvements in SAMs allow a better agreement with observations for the fractions of red satellites once the following considerations are implemented: (i) a decreased stripping efficiency and (ii) a significant loss of low-mass satellites tidally disrupted during the accretion by a central host galaxy (Font et al. 2008; Kang & van den Bosch 2008). Thus, satellite galaxies are able to retain a significant fraction of their hot gas for several Gyr, replenishing their reservoirs of cold, star-forming gas and remaining blue for relatively longer periods of time.

Given that the fraction of red galaxies is a good indicator of the evolutionary state of a group (Bell et al. 2004), we also investigate the variations of this parameter with concentration and isolation in the mock and SDSS groups (Fig. 6). We find that both SDSS and mock groups show a similar trend of increasing red galaxy fraction as a function of concentration (left-hand panel of the figure, significance levels greater than 4σ; Tables 1 and 2). This result is consistent with the expected behaviour since concentration correlates with age for both SDSS and mock groups. However, it is notable the different fractions present in the model and in the SDSS; the former are $\sim$10 per cent larger, in agreement with previous studies that indicate that semi-analytic colours in the Croton et al. (2006) model are systematically redder than SDSS galaxies (Weinmann et al. 2006).[1]

[1] Croton & Farrar (2008) study galaxy colours in voids in the 2dFGRS (Colless et al. 2001), and find that the SAM by Croton et al. (2006) produces similar galaxy colours in such low-density environments. Note that this is not to be compared to our results since in our case, even in the most isolated environment galaxies are embedded in virialized groups of at least 10 galaxy members, i.e. not in galaxy voids.

On the other hand, as can be seen in the right-hand panel of this figure, high-mass SDSS groups show a decreasing fraction of red galaxies as groups become more isolated, in agreement with the larger fraction of late-type galaxies found to populate them (Fig. 3). We calculate how often extremely isolated SDSS massive groups, with distances to their closest neighbours larger than $8R_{\rm vir}$, show red galaxy fractions below the median as a function of Σ_5 and find that this occurs with a frequency of a (70 ± 17) per cent, again with Σ_5 values over the whole range shown in the figure. This is in agreement with the results found for the *M*/*L* dependence on isolation and concentration.

In contrast, as we have already discussed, mock catalogues show that high-mass groups have a larger fraction of red galaxies as the isolation increases. In fact, this disagreement suggests that the SAM fails to reproduce the evolution of galaxy population in the lowest density environments, overestimating the level of ageing. This suggests that the model should include some physical process to stop the reddening of the group/cluster galaxy population in more isolated environments as was discussed previously.

So far, our analysis of SDSS groups proves that at a given concentration the degree of isolation for high-mass groups may play a role at not only determining the number of group members but also at modulating the star formation histories (i.e. high-mass, isolated groups have a smaller fraction of red galaxies). Again, even though the mock catalogues are able to reproduce the dependence of number of members on isolation, they fail to show the observed trend for the red galaxy fraction.

With the purpose of confirming that the galaxy population is intrinsically different for groups of fixed mass and different degrees of concentration and isolation, we estimate the magnitude difference between the brightest and second-brightest group galaxies, ΔM_{12}. As it can be seen in Fig. 7, both the observed and simulated groups show a clear albeit weak tendency for higher values of ΔM_{12} for more concentrated groups (greater than 1σ detections; Tables 1 and 2), indicative of older group ages (Mendes de Oliveira & Carrasco, 2007). In the case of the isolation, as shown in the right-hand panel of Fig. 7 the dependence of ΔM_{12} is similar, although not that clear for massive SDSS groups. These findings suggest that at a given mass, groups show slightly different galaxy populations depending on their concentration and isolation. It is important to recall that for the more massive systems, concentration and isolation are not correlated. Note the higher typical values of ΔM_{12} in the mock

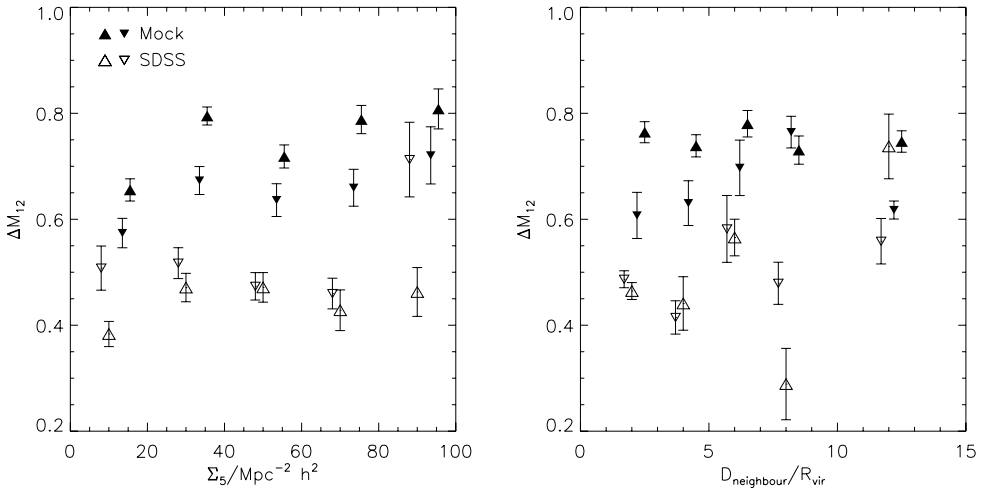

Figure 7. Dependence of ΔM_{12} on group concentration (left-hand panel) and isolation (right-hand panel) for the mock (filled symbols) and SDSS (open symbols) group catalogues. Upward pointing triangles refer to group masses $13.6 < \log_{10}(M_{\rm vir}\, h^{-1}\, {\rm M}_{\odot}) < 14.0$, whereas downward pointing triangles to $12.9 < \log_{10}(M_{r\rm vir}\, h^{-1}\, {\rm M}_{\odot}) < 13.3$.

catalogues suggesting a larger difference between central and satellite galaxies in the model than those in the SDSS. This should be considered a possible problem in the galaxy formation modelling which suggests again an overestimation of the effects of environment in the semi-analytic scheme.

Finally, we studied the variation of group projected shapes on concentration and therefore group age. We were not able to detect any significant variations in this sense for either the mock or SDSS group samples, even though it is expected that older groups or dark matter haloes show rounder intrinsic and apparent shapes (Paz et al. 2006). Note that the analysis was carried out using the same narrow (0.4 dex) ranges of group mass and different concentrations, that according to our mock catalogues should have included groups with ages differing by up to 800 Myr.

5 DISCUSSION

The results found in the previous sections on the effects of isolation and concentration on the properties of groups and galaxy groups can be used to shed light on several aspects of the galaxy formation process, in particular in view of several discrepancies in the behaviour of real and simulated galaxies.

We start by reviewing the results obtained for the mock catalogues. In the mocks, more isolated and concentrated groups, independent of their masses, show almost constant mass-to-light ratios, slightly higher ΔM_{12} and higher red galaxy fractions. With respect to the number of members, mock catalogues show different behaviours; low-mass groups have constant galaxy numbers independent of their concentration or isolation and massive groups show opposing trends of increasing and decreasing number of members as the concentration and isolation increase (i.e. as the age increases), respectively.

On the other hand, high-mass SDSS-DR6 groups show different trends depending on their concentration and isolation. We now analyse high- and low-mass group results separately. (i) For high masses, the most isolated groups are characterized by higher mass-to-light ratios, lower number of members and lower red galaxy fractions as a consequence of being more populated by late-type galaxies. However, as a function of increasing concentration we find lower mass-to-light ratios and higher number of members and red galaxy fractions, in agreement with their older stellar populations as determined by their spectral types. Considering that the group age is proportional to the concentration and anti-correlates with the isolation, the discrepant trends of *M*/*L* and red galaxy fractions in SDSS-DR6 groups suggest different assembly processes indicated by different degrees of concentration and isolation; in particular, the conditions placed by the large-scale structure around groups seems to be important in shaping a group galaxy population such that more isolated groups present lower numbers of galaxies, bluer colours and consequently larger mass-to-light ratios. (ii) For low-mass SDSS groups, trends are more difficult to detect with either concentration or isolation, except for a consistent decrease of *M*/*L* with concentration and isolation (and consistent with the results from the mocks).

As can be seen, the characteristics of galaxy groups in the SAM only reproduce the observations to some level; in particular, massive groups show a dependence of *M*/*L* and red galaxy fraction on isolation and concentration in stark contrast to the observational results. Also, the values of ΔM_{12} and red galaxy fractions are higher than in the SDSS regardless of group mass. These problems may be understood by considering that more isolated groups are older in the model, in contradiction with the results from the observations. This suggests an overestimation of the environmental effects on the evolution of systems, with an excess of old galaxies in the lowest density environments. Particularly, the treatment of satellites in the SAM, which lose their hot gas component and, consequently, their sources of gas accretion when entering into a new dark matter halo, could be responsible for most of the trends observed in the mock groups, including the high values of red galaxy fraction and ΔM_{12}, as well as the lower *M*/*L* values.

The process thought to be responsible for the removal of cold gas from satellites is ram pressure (Haynes & Giovanelli 1986; Solanes et al. 2001, and more recently Brueggen & De Lucia 2007, and references therein), which is considered by some of the current models of semi-analytic galaxy formation to produce an instantaneous result (Cole et al. 2000; Baugh et al. 2005; De Lucia et al. 2006; Croton et al. 2006; Bower et al. 2006; Lagos, Cora & Padilla 2008). Our observational results show several details that could be

used to improve the modelling of processes that drive the evolution of galaxies. For instance, if satellites in isolated groups or clusters were allowed to form stars after being accreted, the fractions of red galaxies and ΔM_{12} values would decrease and the agreement with the observations would improve.

6 CONCLUSIONS

We have searched for possible dependencies of the galaxy population in groups on their assembly history, focusing on possible observational indicators of group age, with the aim of applying the study to the SDSS-DR6 data set.

In order to find indicators of group age, we use mock SDSS group catalogues and find two suitable candidates: (i) the isolation of the group defined as the distance to the nearest neighbour in terms of its virial radius and (ii) the concentration, measured as the density calculated using the fifth closest, bright galaxy to the group centre. Groups within narrow ranges of group mass in the mock catalogue show an increase of group age with isolation and concentration. We also find that the group age is correlated with the luminosity and colour of group galaxies, and with the magnitude difference between the brightest and second-brightest group galaxies.

In order to test if these two theoretical age indicators can also be used in SDSS groups, we analyse the dependence of group spectral types on isolation and concentration finding consistent results only for the latter. Using both the isolation and concentration of galaxy groups as indicators of their assembly history, we study properties of group galaxies in SDSS and mock groups of similar mass. We find important variations in mass-to-light ratios, red galaxy fractions and ΔM_{12}. These correlations or relations are not compatible between model and observations, a problem that can be explained in terms of the differing trends found for age and spectral type as a function of isolation. We discuss how the modelling of the cold gas in satellite galaxies in the SAM could be responsible for these discrepancies.

In this paper, we have confirmed that in addition to a difference in clustering amplitude, groups of similar mass and different assembly histories also show important differences in the characteristics of their member galaxies, an aspect that can be added to current halo model and conditional luminosity functions, and that can also be used to improve the modelling and understanding of the evolutionary processes that shape galaxies in the observed Universe.

ACKNOWLEDGMENTS

We thank the referee for his/her useful comments which have contributed to improve this paper. This work was supported in part by the FONDAP 'Centro de Astrofísica', Fundación Andes, Consejo Nacional de Ciencia y Tecnología (PIP 6446) y Agencia Nacional de Promoción Científica y Técnica (PICT 32342). NP was supported by a Proyecto Fondecyt Regular No. 1071006. This work was supported by the European Commission's ALFA-II programme through its funding of the Latin-american European Network for Astrophysics and Cosmology (LENAC).

REFERENCES

Adelman-McCarthy J. et al., 2007, ApJS, 175, 297
Baugh C. M., Lacey C. G., Frenk C. S., Granato G. L., Silva L., Bressan A., Benson A. J., Cole S., 2005, MNRAS, 356, 1191
Bell E. F. et al., 2004, ApJ, 608, 752
Berlind A. A. et al., 2006, ApJS, 167, 1
Blanton M. et al., 2005, AJ, 129, 256
Blanton M., Berlind A., 2007, ApJ, 664, 791
Bower R. G., Benson A. J., Malbon R., Helly J. C., Frenk C. S., Baugh C. M., Cole S., Lacey C. G., 2006, MNRAS, 370, 645
Brueggen M., De Lucia G., 2007, MNRAS, 383, 1336
Cole S., Lacey C. G., Baugh C. M., Frenk C. S., 2000, MNRAS, 319, 168
Colless M. M. et al., (2dFGRS Team), 2001, MNRAS, 328, 1039
Cooray A., 2005, MNRAS, 364, 303
Cooray A., 2006, MNRAS, 365, 842
Cooray A., Sheth R., 2002, Phys. Rep., 372, 1
Croton D., Farrar G. R., 2008, MNRAS, 386, 2285
Croton D. J. et al., 2006, MNRAS, 365, 11
Croton D., Gao L., White S. D. M., 2007, MNRAS, 374, 1303
De Lucia G., Springel V., White S. D. M., Croton D., Kauffmann G., 2006, MNRAS, 366, 499
Font A. et al., 2008, MNRAS, 389, 1619
Gao L., White S. D. M., 2007, MNRAS, 377, L5
Gao L., Springel V., White S. D. M., 2005, MNRAS, 363, 66
González R. E., Padilla N., Galaz G., Infante L., 2005, MNRAS, 363, 1008
Haynes M., Giovanelli R., 1986, ApJ, 396, 466
Jing Y. P., Suto Y., Mo H. J., 2007, ApJ, 657, 664
Kang X., van den Bosch F., 2008, ApJ, 676, 101
Lagos C., Cora S., Padilla N., 2008, MNRAS, 388, 587
Li Y., Mo H. J., Gao L., 2008, MNRAS, 389, 1419
Mendes de Oliveira C. L., Carrasco E. R., 2007, ApJ, 670, 93
Merchán M., Zandivarez A., 2005, ApJ, 630, 759
Mo H. J., White S. D. M., 1996, MNRAS, 282, 347
O'Mill A., Padilla N., Lambas D., 2008, MNRAS, 389, 1763
Padilla N., Baugh C. M., 2002, MNRAS, 329, 431
Paz D., Lambas D. G., Padilla N., Merchán M., 2006, MNRAS, 366, 1503
Sheth R. K., Mo H. J., Tormen G., 2001, MNRAS, 323, 1
Solanes J. M., Manrique A., Garcia-Gómez C., González-Casado G., Giovanelli R., Haynes M. P., 2001, ApJ, 548, 97
Spergel D. N. et al., 2003, ApJS, 148, 175
Springel V. et al., 2005, Nat, 435, 629
von Benda-Beckmann A., D'Onghia E., Gottloeber S., Hoeft M., Khalatyan A., Klypin A., Müller V., 2008, MNRAS, 386, 2345
Wang Y., Yang X., Mo H. J., van den Bosch F., Weinmann S., Chu Y., 2008, ApJ, 687, 919
Wechsler R., Zentner A., Bullock J., Kravtsov A., Allgood B., 2006, ApJ, 652, 71
Weinmann S. M., van den Bosch F. C., Yang X., Mo H. J., Croton D. J., Moore B., 2006, MNRAS, 372, 1161
Yang X., Mo H. J., van den Bosch F. C., Pasquali A., Cheng L., Barden M., 2007, ApJ, 671, 153
Yip C. et al., 2004, AJ, 128, 585
Zehavi I. et al., 2004, ApJ, 608, 16
Zheng Z. et al., 2005, ApJ, 633, 791

This paper has been typeset from a TEX/LATEX file prepared by the author.